Iran. J. Radiat. Res., 2010; 8 (2): 61-74

Dosimetry limitations and pre-treatment dose profile correction for sliding window IMRT

G. Grigorov[1*], J.C.L. Chow[2], N. Yazdani[1]

[1]Grand River Regional Cancer Center, Grand River Hospital, P.O. Box 9056, 835 King Street West, Kitchener, ON, Canada N2G 1G3

[2]Radiation Medicine Program, Princess Margaret Hospital, 610 University Avenue, Toronto, ON, Canada M5G 2M9

Background: This work investigated the dosimetry limitations of the random and systematic uncertainties of sliding window (SW) intensity modulated radiation therapy (IMRT). ***Materials and Methods:*** A Varian 21EX linear accelerator, Pinnacle^3 treatment planning system and radiographic film dosimetry was used. The limitations of the SW were studied using beam modulation ranging from 2 to 100 MU/beam, DR from 100 to 600 MU min^{-1}, LV from 1 to 5 cm s^{-1} and field size up to 12 × 12 cm^2. The random and systematic errors were investigated using clinical and flat beams, as well as beams of high profile modulation including linear, exponential, and sinusoidal profiles. ***Results:*** The leading edge and plateau of the SW profiles have a significant deformation for higher DR and for beams of < 10 MUs/beam. It was found that the error is directly proportional to the DR and LV, and inversely proportional to the number of MU/beam. ***Conclusion:*** The high DR and LV are limiting factors, producing random profile deformation when SW beams of small number of MU/beam are delivered. A very good agreement was found between the planned and delivered geometrical and clinical dose profiles when beams > 10 MUs irradiated by a DR from 100 to 600 MU min^{-1} and LV from 1 to 5 cm s^{-1}. After the proposed correction, an average difference < 0.5% for clinical profiles was measured for beams irradiated with DR = 600 MU min^{-1} and LV= 5 cm s^{-1}. It was concluded that this correction methodology may serve as a pre-treatment Quality Assurance tool for SW IMRT beams. **Iran. J. Radiat. Res., 2010; 8 (2): 61-74**

Keywords: *IMRT, sliding window, pre-treatment QA and pre-treatment dose correction.*

INTRODUCTION

The delivery of intensity modulated radiation therapy (IMRT) using dynamic multi-leaf collimator (MLC) with variable leaf velocity (LV), constant dose rate (DR), and a method for the conversion of the ideal fluence intensity map to sliding window (SW) leaf trajectory were proposed by Källman *et al.* 1988 [(1)]. Many reports describing the SW technique were then published [(2-14)].

In SW-IMRT, the A and B group of leaves of the MLC (under the X1 and X2 Jaws, respectively) are controlled to move in one direction under the prescribed leaf trajectory or a sequence of control points to produce the required fluence intensity map. A critical point for the SW beams happens at the start of the irradiation, when the DR and LV are equal to zero. With such a short sampling time (about 50 ms), the system has to stabilize the DR and LV and to control the AB leaves' coordinates. Therefore, the DR and LV may not be synchronized during the sampling of the MLC control system when small number of monitor units (MUs) is irradiated. As a result, the SW profile can be affected by certain random dose errors. There is no related dosimetric interlock for a given MU/control point. The total beam dose is monitored and controlled only by the ionization chamber within the head of the linear accelerator. There is no feedback to correct the dose for the SW control points, and the beam control system turns the beam "OFF", when the total planned dose has been reached. During the irradiation, the DR and LV are dynamically controlled. Factors such as nonlinear beam output, scatter, leakage and MLC design may cause

Corresponding author:
Dr. Grigor Grigorov,
Medical Physics Department, Grand River Regional, Cancer Center, PO Box 9056, 835 King St West, Kitchener, ON, Canada N2G 1G3.
E-mail: grigor.grigorov@grhosp.on.ca

a dosimetric and geometric uncertainties of the dose distribution. Since the beam output modeling of the planning system for small fields as well as for asymmetrical and irregular fields depends critically on the linearity of the beam output characteristic, certain disagreements between the calculated and delivered dose distributions can be measured. These factors cause a systematic dose disagreement because they have a static but not dynamic character. Evaluation of the disagreement between the planned and delivered dose is a part of the pre-treatment verification in the Quality Assurance program (QA) of SW-IMRT.

To prevent dose uncertainties of the delivery system the limitation caused by the DR, LV and MU/control point has to be known. A pre-treatment QA program for IMRT plans is provided to compare the calculated and measured dose distributions. Basically, the QA program includes a dose map comparison and checkout of the dose at the isocenter. The dose map calculated for a given plan and buildup by the treatment planning system is compared to that obtained by a 2D dose detector with the same dosimetric setup using radiographic films, portal imager, matrix of ionization chambers (IC) etc. The pre-treatment verification is based on the treatment planning process, including phases such as the checking of the plan optimization, dose map generation for each beam, and its transformation to leaf control points. Although there is no unique relationship between the prescribed dose at a reference point (or to a defined volume) to the number of MU per a given beam, the MU checking is a secure method in the beam QA [15-17]. Using the treatment planning system, every beam is re-projected onto a uniform phantom so that the dose at some reference point(s) can be calculated. Then the dose measured at the same control point(s) and dosimetric setup is compared with the calculated doses. Similarly, the 2D dose distribution of each beam for a given cross section can be verified based on a comparison between the calculated dose distributions in a specific plane with measurements from a 2D dose detector exposed in the same plane. To evaluate the differences between the calculated and measured dose fields, the "gamma method" was used [18, 19]. There are two criteria for accuracy. The first is requirements for highest dosimetric accuracy in regions of low dose gradient. The second is requirements for highest geometric accuracy in regions of high dose gradient. For example, if the criteria are set at 2% and 3 mm, all points are within 2% of the expected dose or are within 3 mm of the nearest point with the expected dose area considered acceptable. These differences are not further used for a correction of the dosimetric/geometric uncertainties for the IMRT beams. The agreement between both maps is provided by a y index. Using a portal image for the y index, agreements within 3% local dose difference, and 3 mm distance were reported [20]. Better results were obtained using an ionization chamber array, which confirms agreement to within 2% of the maximum dose or 2 mm distance for all points within the IMRT fields [21].

The beam profiles delivered by sliding window technique have one characteristic which may serve very well to provide a pre-treatment QA of the IMRT beams, as well as, to correct the in feedback the dose map in the field. Using a 2D dose detector of enough resolution of the dose readings, it is possible to compare dose profile for every leaf pair to the dose profile calculated by the planning system for the same pair. More over, if any systematic dose uncertainty is discovered addressing one or more leaf pairs, the control points of the affected leaf pairs can be modified directly in their control code using a dose correction matrix

Beam profiles of rectangular, sinusoidal, exponential and linear shapes, as well as clinical beams were used to determine the range of the random and systematic dose errors for SW beams. To investigate the mechanical and dosimetry characteristics of the MLC, its leakage component and

the SW beam delivery time, beams from 2 to 100 MU were irradiated with a DR up to 600 MU min^{-1} and LV up to 5 cm s^{-1}. Measurements were performed using a Varian 21EX linear accelerator and Kodak XV–Omat radiographic film dosimetry. In Grand River Hospital, our treatment planning system is currently not equipped with software to convert ideal fluence maps to SW-MLC sequences. To study dose inaccuracies of SW profiles, an in-house software (SWIMRT) built on the MATLAB® v. 7.1 platform was used [9]. It should be noted that this software has not included a dose correction regarding the small fields beam output, scatter and leaf design produced by the specificity of the Varian MLC. As the delivery time of the SW beams is an important parameter, the possibility to irradiate the SW beams using the extreme DR and LV was also investigated.

It was found that the random and systematic profile uncertainties affect the leading edge and plateau of the SW profiles, and the dose magnitude of the control points, respectively. In this study, we found out for which combination among the DR, LV and MU/beam, the random profile uncertainties can be avoided. As the multiple measured systematic dose errors from one and the same beam were found to have equivalent values from same control points, it was assumed that these errors could be corrected. The evaluation of the dosimetric/geometric uncertainties between the calculated and measured fields was based on calculation grid with a step of 0.1 mm. A 2D dose error profile was generated using all leaf pairs. As a final step in the pre-treatment dose profile verification, we used the 2D dose error profile in a feedback to correct the leaf trajectory directly in the MLC code without rerunning the optimization algorithm. The MU correction of the control points included in an integrated dosimetric uncertainty caused by the beam output, leaf design, scatter and so on. After the correction, an average deviation < 0.5% was measured for the used clinical beams irradiated with the extreme DR and LV.

MATERIALS AND METHODS

Dosimetric equipment and measurements

The limitations of the SW-IMRT dose delivery were studied using the 6 MV photon beams for clinical and non-clinical cases. SW beams with dose modulation ranging from 2 to 100 MU/beam were irradiated in the X1→ X2 leaf pair direction and delivered to a Solid Water phantom using a DR from 100 to 600 MU min^{-1} and LV from 1 to 5 cm s^{-1}. The beams for clinical case were initially calculated for a step-and-shoot IMRT using Pinnacle^3 treatment planning system and then converted to SW beams using our SWIMRT software.

The beams for non-clinical cases of flat, linear, exponential and sinusoidal shape were generated by the SWIMRT and SHAPER program (v 6.2, Varian Medical Instruments Inc.) as *.mlc* files. The measurements were performed using a Varian Clinac 21 EX linear accelerator, (Varian Medical Systems, Palo Alto, CA) equipped with a 120-leaf Millennium MLC. In this study, the profiles are shown in figures as follows: the initially planned profiles are in black, the profiles irradiated before the correction are in pink, the corrected profiles are in blue, and the delivered profiles after correction are in red.

The profile uncertainties of the SW beams for clinical case were evaluated by comparing the dose profile calculated from Pinnacle^3 to a plane at a given depth in a flat water phantom to a dose profile obtained by radiographic film using the same experimental configuration. The planar and film dose maps of every beam exported as ASCII format were analyzed using the OmniPro™ I'mRT, v. 1.5 (SCANDITRONIX WELLHOFER). It was assumed that the dose error for every control point includes an individual differential dose component caused by the beam output, scatter, trans-

mission, tongue-and-groove effect, MLC design and so on. The differential values were calculated using Microsoft® Office Excel 2003 and exported to the SWIMRT to rescale the initial shape of the SW profile. The initial, planned and the corrected profiles were compared graphically.

The dose profiles were measured in a Solid Water phantom (30 × 30 × 30 cm^3) at the central axes, source-to-axis distance (SAD) = 100 cm, and in a specific depth using film dosimetry. The films were processed with a Kodak X–Omat 2000 film processor in a single batch. Developed films were scanned using a 16–bit Vidar VXR–16 film scanner (Vidar Systems Corp., Herndon, VA) and analyzed using the RIT 113V4 software (Radiological Imaging Technology, Inc., Colorado Springs). The optical density to dose conversion was performed using a MLC file generated by the SHAPER program for step irradiations of films. A cubic-spline algorithm was used to fit the optical density calibration function. The calibration curve was obtained according to the instructions of the RIT system. MLC fields with 13 equal dose steps within the range of sensitivity of Kodak films were used for the film calibration. For the day of measurements, doses obtained by radiographic films were rescaled additionally by readings obtained by a farmer chamber for 100 MUs of 6 MV photon beam, at 5 cm depth of Solid Water phantom, field size = 10 × 10 cm^2 and source-to-surface distance (SSD) = 95 cm using a calibrated ionization chamber.

Geometrical beam profiles

The random dose profile uncertainties were studied using SW beams of flat profile with field sizes of 5 and 10 cm in the X2 - direction and from 2 to 10 MU/beam. A comparison between the static and SW beams of the same experimental setup was carried out to determine the agreement between the planned and delivered SW profiles. The curves in figures 1-3, obtained with TL films at depth of 5 cm, are for beams irradiated by a DR = 100, 400 and 600 MU min^{-1} and LV = 1, 3 and 5 cm s^{-1}.

The systematic profile deviation was studied using beams with a dose modulation ranging from 10 to 100 cGy. The profiles of linear ($y = a + b \times x$), exponential ($y = a + c / \exp(x)$) and one and two sinusoidal ($y = a + d.\ \sin(p\ .\ x)$ and $y = a + f.\ \sin(2p\ .\ x)$) dose gradient modulation (see figures 4, 5 and 8 (a-d)) mimic closely the graphical elements of the clinical dose profiles. The equations had specific coefficients of *a* to *f* (from *a* = 10 and *b* to *f* from 10 to 100 cGy) to fit a field of x = –6 to +6 cm from the central beam axis. Each profile represents a superposition of two dose distributions. One has 10 MUs and another has the corresponding geometric shape with a maximum of 90 MUs. A specific number of MUs = 124, 124, 169 and 259 MU/beam for the linear, exponential and one and two sinusoidal profiles, respectively were used to deliver at a depth of 5 cm the prescribed dose profiles with a DR = 600 MU min^{-1} and LV = 5 cm s^{-1}. Five measurements were carried out for each geometric profile.

Clinical beams

IMRT plans of two randomly selected patients, diagnosed with prostate (figure 6) and head-and-neck cancer (figure 7), were used to study the random and systematic dose profile uncertainties for the SW dose delivery. Patients were scanned in the target area with an AcQSim CT scanner (Philips Medical Systems Inc, Cleveland). The planning target volumes (PTVs) and organs at risk (OARs) were outlined according to the guidelines in the Radiation Therapy Oncology Group studies [22, 23].

A prescribed fractional dose of 82 Gy/41 with 5 beams and 60 Gy/30 with 11 beams of 6 MV photon beams were used for the plan optimization for the prostate and the head-and-neck plan, respectively. Initially, plans were optimized for step-and-shoot IMRT using the Pinnacle³ v. 7.4 (Philips Medical Systems, Milpitas, CA). Then every beam was recalculated in the

planning system using zero beam gantry angle, with SAD = 100 cm and reference depths (12 and 5 cm for prostate and head-and-neck, respectively) in a Solid Water phantom. To avoid the dose redistribution caused by the overshoot effect and positional errors in the reference step-and-shoot beams, radiographic films were irradiated using a DR = 100 MU min^{-1} [24- 26]. The step-and-shoot beams were converted to SW beams using the SWIMRT software, and irradiated for the same experimental configuration. The total delivery time for the step-and-shoot and SW-IMRT, and the MU/beam are shown in tables 1 and 2.

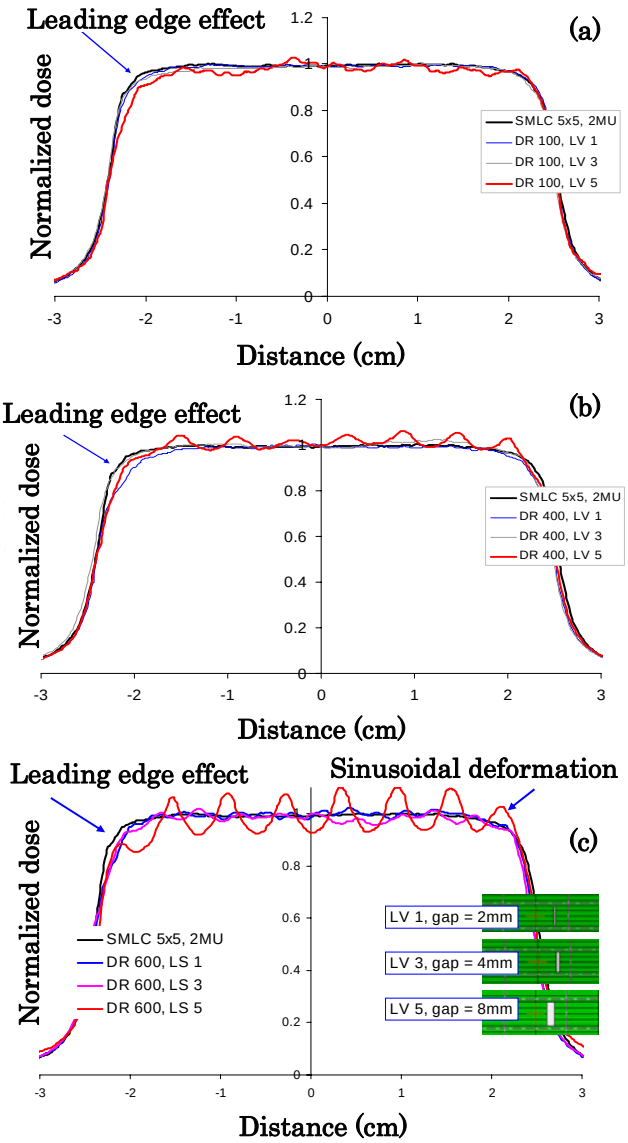

Figure 1. Sliding window beam profiles for field length of 5 cm, 2 MU/beam, 6 MV photon beam delivered with LV = 1, 3 and 5 cm s^{-1}: (a) DR = 100 MU min^{-1}, (b) DR = 400 MU min^{-1} and (c) DR = 600 MU min^{-1}.

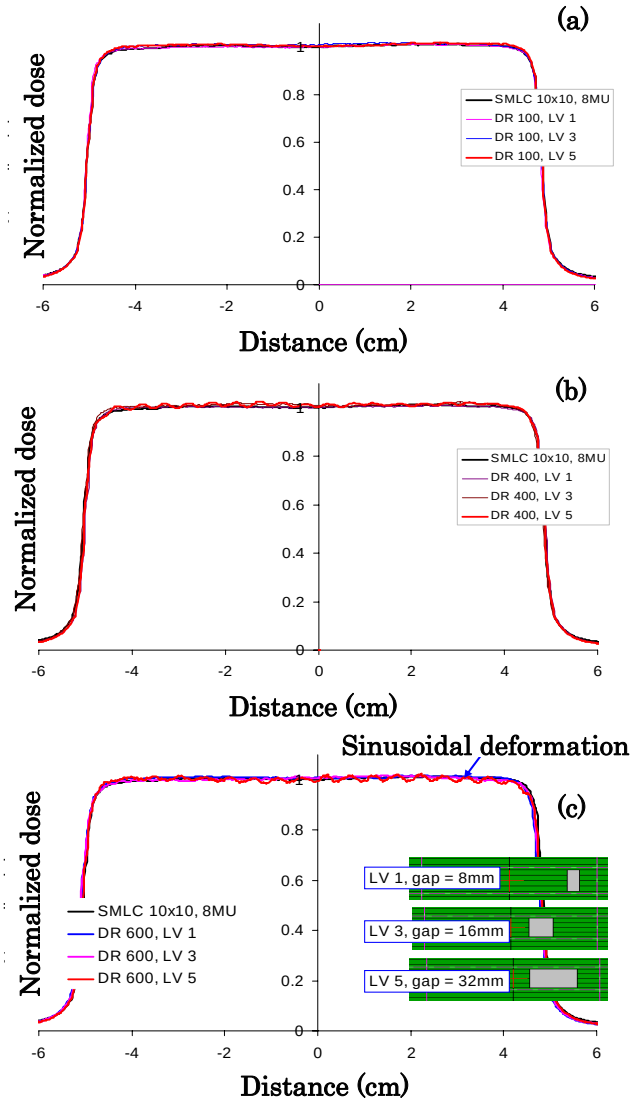

Figure 2. Sliding window beam profiles for field length of 10 cm, 8 MU/beam, 6 MV photon beam delivered with LV = 1, 3 and 5 cm s^{-1}: (**a**) DR = 100 MU min^{-1}, (**b**) DR = 400 MU min^{-1} and (**c**) DR = 600 MU min^{-1}

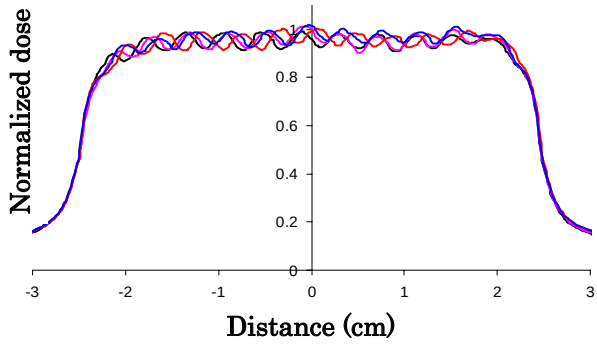

Figure 3. Sinusoidal Random dose inaccuracy of the plateau for SW beam of 3 MUs, field length of 5 cm, DR = 600 MU min^{-1}, LV= 5 cm s^{-1}.

Table 1. Comparison of the total delivery times for the prostate IMRT beams.

S&S IMRT			SW IMRT								
Leaf Speed [cm s^{-1}]	0		1	3	5	1	3	5	1	3	5
Planned MU	130		149	136	134	207	156	145	246	169	153
100 MU/min	Time [s]	78	89.4	81.6	80.4	-	-	-	-	-	-
400 MU/min		19.5	-	-	-	31.5	23.4	21.7	-	-	-
600 MU/min		13	-	-	-	-	-	-	24.6	16.9	**15.3**

Table 2. Comparison of the total delivery times for the head and neck IMRT beams.

S&S IMRT			SW IMRT								
Leaf Speed [cm s^{-1}]	0		1	3	5	1	3	5	1	3	5
Planned MU	113		137	121	118	208	145	132	257	161	142
100 MU/min	Time [s]	67.8	82.2	72.6	70.8	-	-	-	-	-	-
400 MU/min		17	-	-	-	31.2	21.7	19.8	-	-	-
600 MU/min		11.3	-	-	-	-	-	-	25.7	16.1	**14.2**

Dose profile correction matrix

Let y_1 be the original planned dose profile for a given leaf pair calculated for the Solid Water phantom and y_2 be the dose profile delivered by the SW beam and measured in a Solid Water phantom for the same leaf pair and experimental configuration. The profile y_2 represents the sum of the planned dose and dose uncertainties. It was assumed that the difference between y_1 and y_2 may be used as a correction function (CF) to correct the systematic beam uncertainties. To calculate the CF, an equal step, x_i = 0.1 mm was used. For example, a field length of 10 cm for the CF has 1000 steps (i = 1 to 1000) per every leaf pair. The CF for one leaf pair was defined as:

$$CF(x_i) = 2 \times y_1(x_i) - y_2(x_i), \qquad (1)$$

The CF for all leaf pairs included in the SW beam may be prescribed as a matrix CF [n, i], where n = 1 to 60 is the order number of the leaf pair and i = 1 to m is the order number of the leaf control points.

The mean value and standard deviation were calculated for every control point of the SW profiles.

RESULTS

Deformation of sliding window beam profiles

The rectangular profiles in figures 1 and 2 were measured for SW fields of 2 × 5 cm^2 with 2 and 3 MU/beam and a field size of 2 × 10 cm^2 and 8 MU/beam, respectively. The profiles in figure 3 are for SW fields of 2 × 5 cm^2. The longer side of the field is in the x-direction. Profiles of static beams with the same field size and MU were used as reference beams here. The SW dose profiles were normalized to the dose at the central beam axis obtained for the corresponding static field size. The leading edge and plateau of the SW profiles in figures 1(b), 1(c) and 2 have a significant deformation for a DR = 400 and 600 MU min^{-1}. The magnitude of the sinusoidal waves of the plateau is about 7 and 15% from the beam dose irradiated with a DR = 400 and 600 MU min^{-1}, respectively. The number of periods may increase proportionally in the length of the field. In figure 2(c), the plateau has about 18 sinusoidal periods and a delivery time of 23 s for

length = 10 cm, and it results in about 1.3 s per period. The SW field sizes for 5 and 10 cm length of the field calculated by the SWIMRT for DR = 600 MU min^{-1} and LV = 1, 3 and 5 cm s^{-1} are shown in figure 1(c) and 2(c), respectively. In the same figures, a gap from 2 to 8 mm and from 8 to 32 mm was calculated to deliver SW profiles, respectively.

To investigate the ability of the MLC to control the DR and LV for low number of MU/beam, one and the same SW beam with DR of 600 MU min^{-1} and LV of 5 cm s^{-1}were irradiated several times on different films. In figure 3, the plateau of every profile has sinusoidal deformation. Additionally, the plateau has a random phase shift of periodic modulations and each of them has with about 20% relative error to the prescribed MU.

In figure 2, the magnitude of random errors in the leading edge and the plateau is directly proportional to the DR and LV and inversely proportional to the number of MU/beam (see figure 2). The deformation of the edge and plateau measured for a beam of 8 MU/beam, DR = 600 MU min^{-1} and LV= 5 cm s^{-1} is significantly lower in comparison to the deformations of the beam of 2 MU/beam irradiated with the same DR and LV (figure 1).

SW beam profiles of single and multiple dose gradients

The linear, exponential and sinusoidal SW profiles irradiated by the 6 MV photon beams, DR = 600 MU min^{-1}, LV = 1 – 5 cm s^{-1} in a Solid Water phantom at SAD = 100 cm, and depth = 5 cm are plotted in figure 4. Each profile was irradiated 5 times. In the sub-figures of figure 4, five identical dose profiles are plotted. A comparison between the planned (reference) geometric curves and the beam profiles without correction, for field size = 12 × 12 cm^2 irradiated with DR = 600 MU min^{-1} and LV = 5 cm s^{-1} is shown in

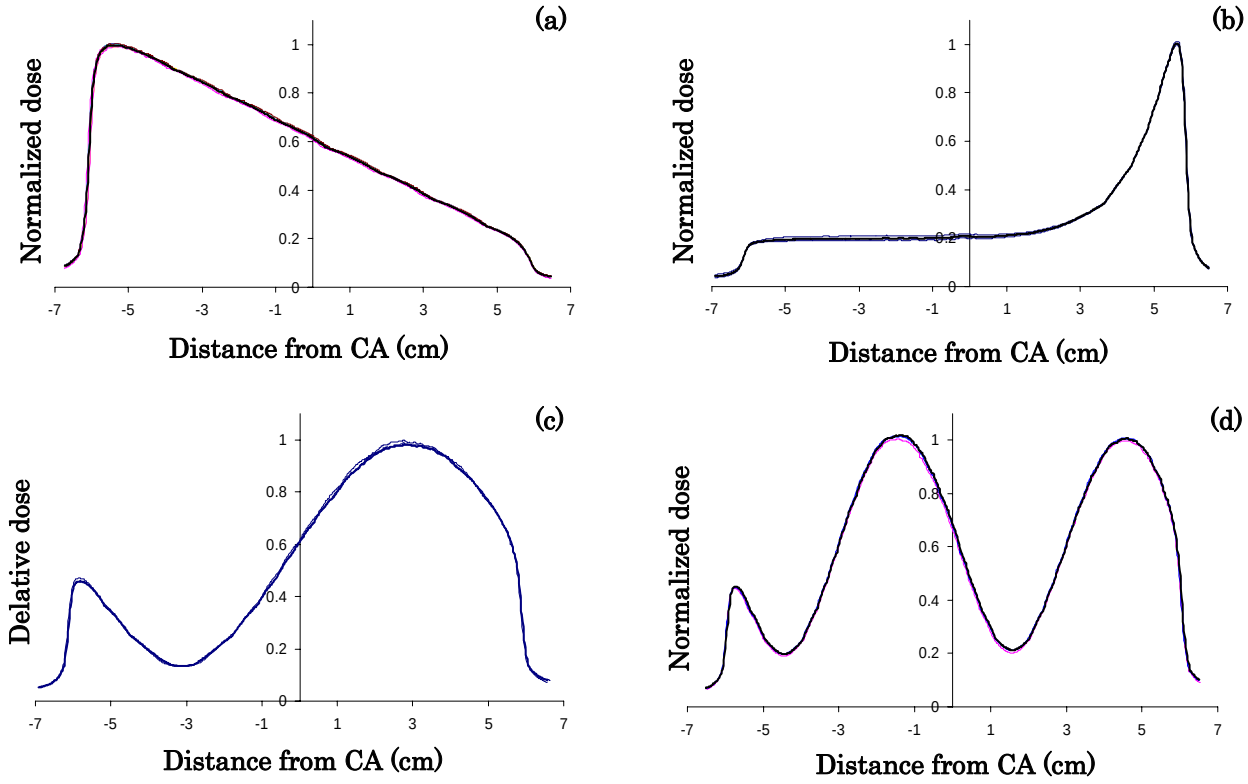

Figure 4. Sliding window profiles delivered in the X1→X2 direction for field size = 12 × 2 cm^2 irradiated by a 6 MV photon beam, DR = 100 – 600 MU min^{-1}, LV = 1 – 5 cm s^{-1} in a Solid Water phantom at SAD = 100 cm and depth = 5 cm: (a) linear; (b) exponential; (c) one sinusoidal period for 12 cm; and (d) two sinusoidal periods for the same X1 - X2 length of the field.

figure 5. A significant non-uniform disagreement between the planned and delivered dose profiles is shown in figures 5 (a-d). All delivered fields have the existence of point (s) of intersection marking the places, where the planned and delivered doses are equal. The points are shown in figure 5 with circles. A systematic difference was measured in more than two hundred SW profiles of different shapes, irradiated under variety of combinations of DR, LV and profile shapes. As the shape of the delivered dose profiles was identical, we assumed that an individual correction factor could be used for every leaf control point. The string of the correction factors per one leaf pair creates the CF, for this particular pair.

Clinical DMLC beams

The treatment times for prostate and head-and-neck SW beams are shown in tables 1 and 2, respectively. The shortest beam-on time of 15.3 and 14.2 s for a DR = 600 MU min^{-1} and LV = 5 cm s^{-1} (see shadow cells in the tables) were calculated for the prostate and head-and-neck beams, respectively.

Prostate IMRT beam

The planned and delivered beam fluence and profile along the X1-X2 axis are shown in figures 6(a) and 6(b). Two non-uniform windows for SW-IMRT correspond to control points of 20% and 80% of the prescribed MU/beam are shown in figure 6.

The dose profiles of the static MLC (used for a reference) and dynamic MLC irradiated with DR = 100 MU min^{-1} (black) and 600 MU min^{-1} (pink) with LV = 5 cm s^{-1}, respectively are shown in figure 8(e). The static and dynamic anterior-posterior beams were irradiated using 130 and 153 MU/beam, respectively. The dynamic profiles have about 5% difference in the plateau of the profile.

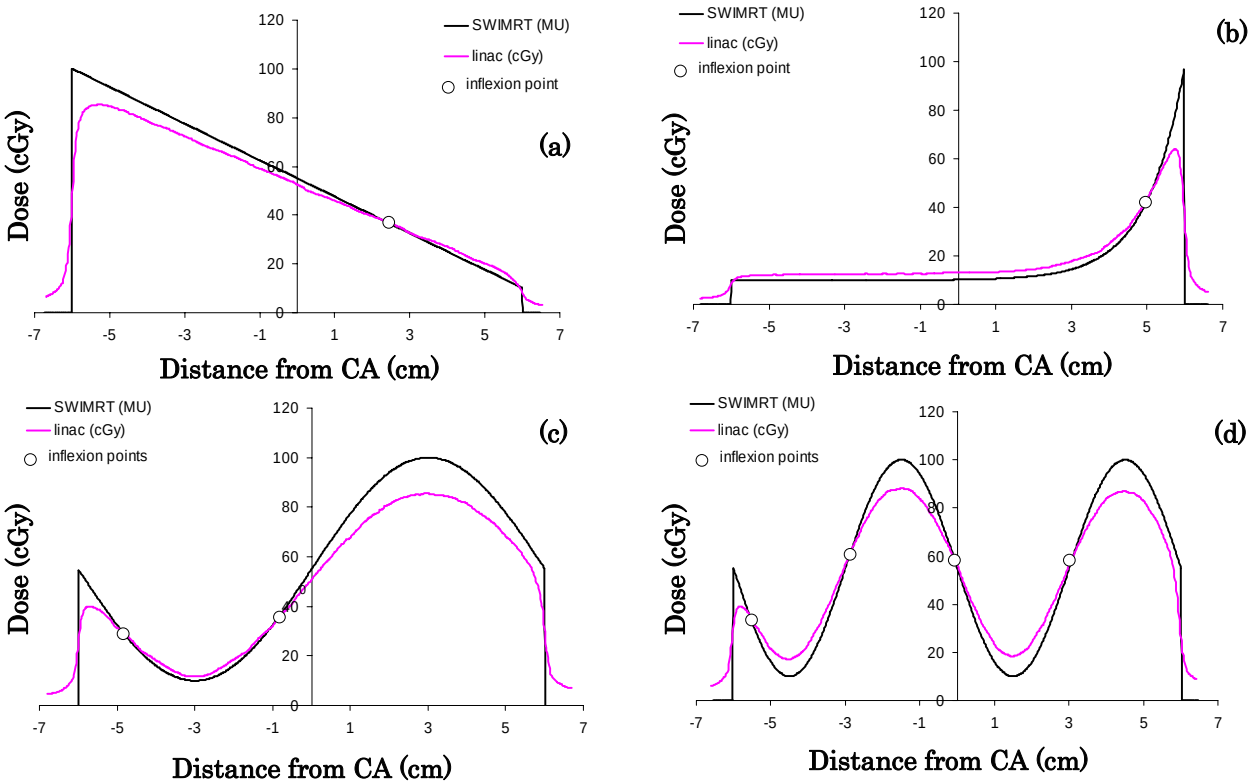

Figure 5. Dose differences between the planned (reference) geometric curves and delivered SW beam profiles without correction, for field size = 12 × 2 cm^2 irradiated with DR = 600 MU min^{-1} and LV = 5 cm s^{-1}. The planned beam profiles are plotted in black. The delivered dose profiles are plotted in pink.

Head-and-neck IMRT beam

Figures 7 (a) and 7(b) show similar information for the head-and-neck beams. The planned and delivered beam fluence for one IMRT beam and profile along the X1-X2 axis is shown in figure 7. The irregular windows in figure 7 correspond to the 20% and 50% of the prescribed MU/beam (figures 7 (c) and (d)). The dose profiles of the static MLC and dynamic MLC irradiated with DR = 100 MU min^{-1} (black) and 600 MU min^{-1} (pink) with LV = 5 cm s^{-1}, respectively are shown in figure 8(f). The static and dynamic beams were irradiated using 113 and 142 MU/beam, respectively. As profile differences are not equal (about 4% - 6%), the correction requires a non-uniform CF for the MLC control points.

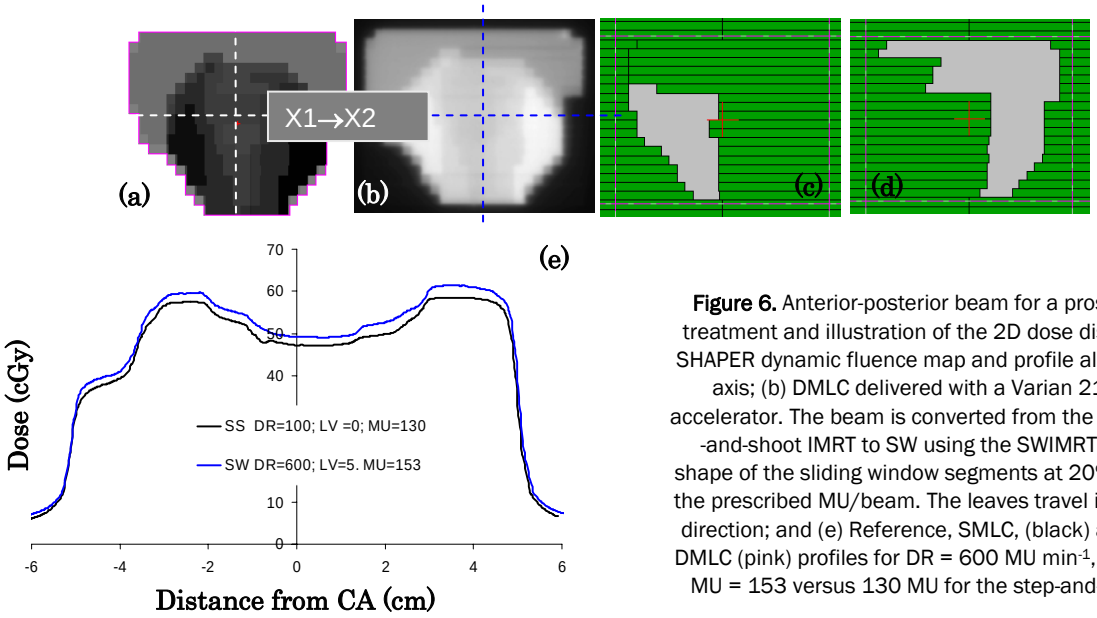

Figure 6. Anterior-posterior beam for a prostate cancer treatment and illustration of the 2D dose distribution: (a) SHAPER dynamic fluence map and profile along the X1-X2 axis; (b) DMLC delivered with a Varian 21 EX linear accelerator. The beam is converted from the Pinnacle^3 step -and-shoot IMRT to SW using the SWIMRT; (c) and (d) shape of the sliding window segments at 20%, and 80% of the prescribed MU/beam. The leaves travel in the X1 ® X2 direction; and (e) Reference, SMLC, (black) and delivered DMLC (pink) profiles for DR = 600 MU min^{-1}, LV = 5 cm s^{-1}, MU = 153 versus 130 MU for the step-and-shoot IMRT.

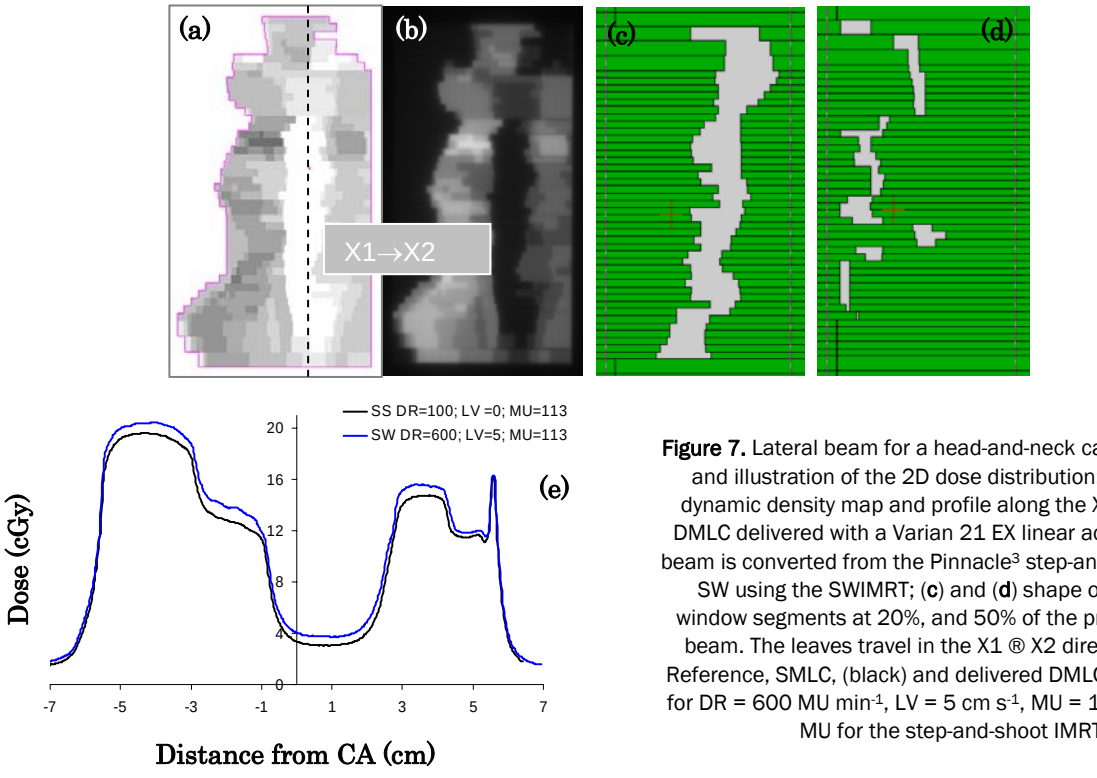

Figure 7. Lateral beam for a head-and-neck cancer treatment and illustration of the 2D dose distribution: (**a**) SHAPER dynamic density map and profile along the X1-X2 axis; (**b**) DMLC delivered with a Varian 21 EX linear accelerator. The beam is converted from the Pinnacle^3 step-and-shoot IMRT to SW using the SWIMRT; (**c**) and (**d**) shape of the sliding window segments at 20%, and 50% of the prescribed MU/ beam. The leaves travel in the X1 ® X2 direction; and (**e**) Reference, SMLC, (black) and delivered DMLC (pink) profiles for DR = 600 MU min^{-1}, LV = 5 cm s^{-1}, MU = 142 versus 113 MU for the step-and-shoot IMRT.

Decreasing the total delivery time is an important objective due to possible effects of internal organ motion and patient movement. Using extreme DR and LV the clinical beams (prostate and head-and-neck) were delivered after corrections for 14.8 s and 13.9 s, respectively. At the same time the value of the leakage outside both fields increased insignificantly from 2.6 to 3 cGy and from 2.2 to 2.8 cGy, respectively in comparison to the SW-IMRT beams. The obtained values are similar to values of the leakage and beam-on times for the step-and-shoot technique for both clinical beams.

Correction methodology for SW beams using a dose profile correction function

The reference profiles, the profiles delivered without any dose correction, the required profiles to deliver planned dose and profiles after the correction are plotted in figure 8. The plots in black correspond to

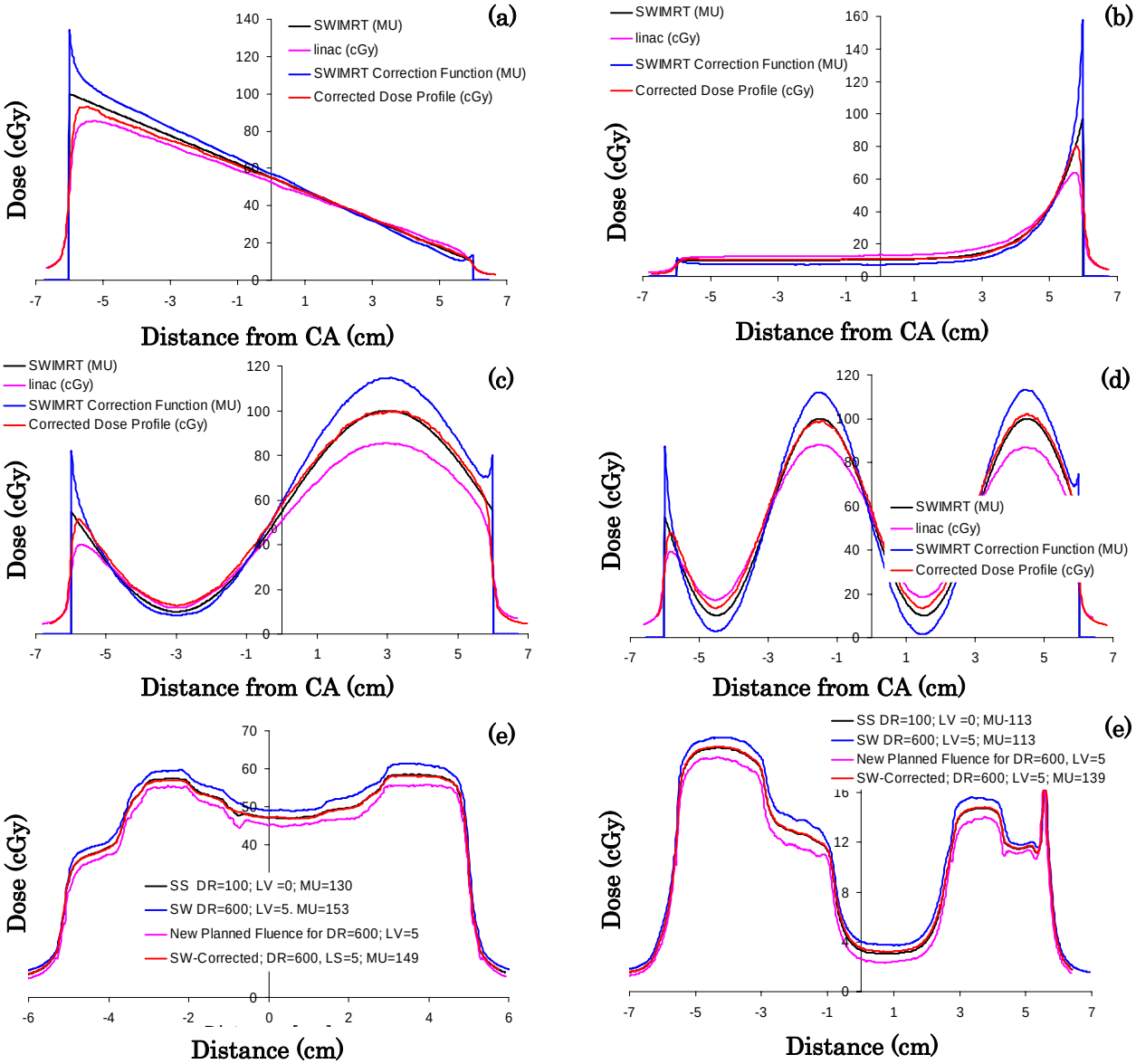

Figure 8. Illustrations of the agreement between the planned and corrected beams. A difference < 0.8% and < 0.5% was achieved for the geometrical and clinical beams, respectively. Geometrical profiles (a-d) are generated using the SWIMRT software. The clinical beams (e-f) were optimized by the step-and-shoot IMRT with Pinnacle³ and converted using the SWIMRT to DMLC. Both beams were corrected using the SWIMRT and delivered using the Varian 21 EX linear accelerator with DR = 600 MU min^{-1} and LV = 5 cm s^{-1}.

the linear, exponential and sinusoidal equations and to the planned clinical step-and-shoot IMRT beams for prostate and head-and-neck treatment. For every beam, the required correction of the dose/control point was determined using equation 1. The new values for the corrected MU/beam are shown in table 3. A significant improvement of the agreement between the planned and delivered geometrical dose profiles was measured after the correction. A maximum dose error < 0.8% was measured in the local maxima of the dose gradients for the geometrical curves.

The corrected clinical beams were irradiated with higher profile accuracy than the non-clinical beams because their dose gradients were smoother. A very good agreement between the planned and delivered profiles of the clinical beams is shown in figures 5(e) and 5(f). The calculated mean value and its standard deviation for the linear, exponential, one sinusoidal, two sinusoidal geometrical beams and the prostate and head-and-neck SW beams are plotted in table 4. The maximum dose error (up to 7%) was measured for edges of the sinusoidal profiles. Minimal average dose error < 0.5%, was found for the exponential and clinical beams.

DISCUSSION

Random dose profile uncertainties depend on the ability of the MLC to control and keep the DR and LV constant when a beam of lower number of MU/beam is used. The deformation of the leading edge and the plateau has emphatically random character. These errors can be avoided only using lower DR and LV.

From other side, the systematic profile uncertainties can be compensated. It was found that, the beams of flat profile a rescaling dose factor of one sign can be used to correct the dose uncertainties. Beams of

Table 3. A comparison between the planned and corrected MUs/beam.

Profile	DR = 600 MU min^{-1} LS = 5 cm s^{-1}		
		Planned DMLC	Corrected DMLC
Linear	MUs/beam	124	163
Exponential		124	189
One sinusoid		169	230
Two sinusoids		259	340
Prostate		149	152
Head and Neck		138	142

Table 4. A comparison between (μ and σ) of the dose error for geometrical and the clinical beams. A maximum dose error in the range from 5 to 11.5% was measured only for edges of the mathematically calculated and delivered sinusoidal, linear and exponential profiles. At the field for all beams, the dose error was less than 1%.

Profile	DR = 600 MU min^{-1} LS = 5 cm s^{-1}		
	μ	σ	Maximum
Linear	0.49	0.74	10.2
Exponential	0.48	0.45	11.5
One sinusoid	0.48	0.33	5.5
Two sinusoids	0.56	0.45	7.1
Prostate	0.32	0.58	<1
Head and Neck	0.24	0.38	<1

high profile modulation may need an individual rescaling factor of different sign for every control point of the SW beam or an individual correction matrix (CF [*n*, **i**]) for a given beam.

To deliver a beam profile of high doze modulation, the SW technique uses sliding gaps of irregular (see figures 6 (c) and (d) and figures 7 (c) and (d) and a small distance of several mm (see figures 1(c) and 2(c)) between the A and B leaves. To measure the beam output or to calculate SW dose profile using monte carlo (MC) simulation is practically very tedious or extremely time-consuming. To calculate one of the used geometrical profiles with a corresponding accuracy, a MC simulation of about 1000 phase space files equal to the number of applied MLC control points has to be used. In this work, the strategy of the correction methodology of the systematic dose uncertainties was based on the difference between the planned and delivered dose profile. Since our software, SWIMRT, does not include any correction related to the beam output and dose inaccuracies caused by the MLC system, it is possible to expect some differences between the profiles calculated with SWIMRT and other commercial or *in-house* programs. We suppose that certain differences between data calculated with commercial and SW beams could be found. A difference could also be found if the SWIMRT is used with other linear accelerators or MLC systems.

To obtain the dose profiles a 2D detector is needed. As the current portal imager (PI) and the 2D matrix are equipped with s semiconductors and ionization chambers have lower resolution than the radiographic films we did not use them in our study. Another reason not to use the PI is related to the impossibility to setup Solid Water slabs over it.

As the measurement of the output for small regular and symmetrical filed sizes below 2 × 2 cm^2 is a known dosimetric problem. In SW beams the gap between the A and B leaf pears can be significantly smaller than 2 cm. As shown in figure 7(d) the smallest gap about 2-3 mm. It is still not solved how routinely to measure the beam output for so small fields and provide QA of the planned beams. In our study, we used another strategy for correction of the dose uncertainties for the SW dose profiles. In our model the integrated difference between the planned and delivered profiles are used as a feedback to correct the SW beams. This model seems to work well though some of the SW control points between leaves A and B are asymmetrical with irregular gaps of only several mm. Using this strategy a very good coincidence between planned and delivered SW profiles was achieved over the entire range of the dose profiles and extreme DR and LV values. Although the correction methodology has been demonstrated by comparison of beam profiles obtained with film dosimetry at a Solid Water phantom of flat surface to dose profiles obtained in the planning system for the same phantom, we assume that the idea to use the function, CF [*n*, *i*] has a potential to serve as a powerful tool for a general QA program for pre-treatment QA of the SW-IMRT beams. The comparison between initially planned and the corrected profiles measured for the same setup profiles (see figures 8(a-f)) show that the correction methodology is effective, over the entire dose and field size ranges and extreme DR and LV.

In the current algorithm, the feed back correction have been applied sequentially from beam-to-beam, that is: 1) the optimization of the required fluence intensity map of the beams; 2) recalculation of the beam profile produced with the same fluence in to a flat Solid Water phantom; 3)irradiation of the calculated beams to the same phantom setup; 4) calculation of the CF [*n i*] as a difference between the dose profiles obtained at the isocenter of the point 2 and 3; and 5) feed back correction of the initial beams using the correction function.

The exploring of the idea to provide not

only a pre-treatment QA of the beam dose modulation but also to use the profile of the systematic dose uncertainties for a pre-treatment dose correction may inspire the colleagues who design planning systems, QA programs and MLC control to establish a clinically relevant pre-treatment dose profile correction .

CONCLUSION

The high dose rate and leaf velocity are limiting factors, producing random profile deformation, when SW-IMRT beams of small number of MU/beam are delivered. It was found that there is a very good agreement between the planned and delivered geometrical and clinical dose profiles, when beams > 10 MUs irradiated by a DR from 100 to 600 MU min^{-1} and LV from 1 to 5 cm s^{-1}. After the correction, an average difference < 0.5% for clinical profiles was measured for beams irradiated with DR = 600 MU min^{-1} and LV= 5 cm s^{-1}. It is concluded that this method can provide a quick, inexpensive and effective feedback correction of the leaf control points so as to deliver SW profiles with higher agreement between the planned and delivered profiles. Although this study was based on the *in-house* developed software, our results suggest that this correction methodology may serve as a pre-treatment Quality Assurance tool for SW-IMRT beams and to provide more precisely dose delivery employing using the correction function CF [*n i*] as a pre-treatment dose correction tool.

ACKNOWLEGMENTS

The study was supported by the Medical Physics Department at the Grand River Regional Cancer Centre. We would like to thank Rob Barnett, Mariusz Ogrodowczyk and John Ukos.

REFERENCES

1. Källman P, Lind B, Eklof A, Brahme A (1988) Shaping of arbitrary dose distributions by dynamic multileaf collimation. *Phys Med Biol,* ***33:*** *1291–1300.*
2. Convery DJ and Rosenbloom ME (1992) The generation of intensity-modulated fields for conformal radiotherapy by dynamic collimation. *Phys Med Biol,* ***37:****1359–1374.*
3. Spirou SV and Chui CS (1994) Generation of arbitrary intensity profiles by dynamic jaws or multileaf collimators *Med Phys,* ***21:*** *1031–1041.*
4. Stein J, Bortfeld T, Dorschel B, Schegel W (1994) Dynamic X-ray compensation for conformal radiotherapy by means of multileaf collimation. *Radiother Oncol,* ***32:*** *163–167.*
5. Chui CS, LoSasso T, Spirou S (1994) Dose calculation for photon beams with intensity modulation generated by dynamic jaw or multileaf collimations*. Med Phys,* ***21****: 1237–1244.*
6. Boyer A and Strait J (1997) Delivery of intensity modulated treatments with dynamic multileaf collimator. Proc. 12th Int. Conf. on the use of computers in radiation therapy (Salt Lake City, Utah 1997) Leavitt DD, Starkschall G, editors. Madison WI: *Medical Physics Publishing, 13-16.*
7. Ma L, Boyer A, Xing L, Ma C-M (1998) An optimized leaf-setting algorithm for beam intensity modulation using dynamic multileaf collimators. *Phys Med Biol,* ***43:*** *1629 –1643.*
8. Dirkx MLP, Heijmen BJM, van Santvoort JPC (1998) Leaf trajectory calculation for dynamic multileaf collimation to realize optimized fluence profiles *Phys Med Biol,* ***43:*** *1171–1184.*
9. Chow J, Grigorov G, Yazdani N (2006) SWIMRT: A graphical user interface using the sliding window algorithm to construct a fluence map machine file. *Jour of Appl Clin Med Physm,* ***7:*** *69-85.*
10. Convery DJ and Webb S (1998) Generation of discrete beam-intensity modulation by dynamic multileaf collimation under minimum leaf separation constraints. *Phys Med Biol,* ***43:*** *2521–3821.*
11. Webb S (2001) Intensity modulated radiation therapy. Bristol: Institute of Physics Publishing, UK.
12. Low DA, Sohn JW, Klein EE, Markman J, Mutic S, Dempsey JF (2001) Characterization of a commercial multileaf collimator used for intensity modulated radiation therapy. *Med Phys,* ***28:*** *752–756.*
13. Litzenberg DW, Moran JM, Fraass BA (2002) Incorporation of realistic delivery limitations into dynamic MLC treatment delivery. *Med Phys,* ***29****: 810–820.*
14. Kamath S, Sartaj S, Palta J, Sanjay R (2004) Algorithms for optimal sequencing of dynamic multileaf collimators, *Phys Med Biol,* ***49:*** *33–54.*
15. Williams P (2003) IMRT: delivery techniques and quality assurance. *British Journal of Radiology,* ***76:*** *766–776.*
16. Van Esch A, Bohsung J, Sorvari P, Tenhunen M, Paiusco M, Iori M, Engström P, Nyström H, Huyskens DP. (2002) Acceptance tests and quality control (QC) procedures for the clinical implementation of intensity modulated radiotherapy (IMRT) using inverse planning and the sliding window technique; experince from five radiotherapy departments. *Radiother Oncol,* ***65:*** *53–70.*
17. Kung J, Chen G, Kuchnir F (2000) A monitor unit verification calculation in intensity modulated radiotherapy as a dosimetry quality assurance. *Med Phys,* ***27:*** *2226-2230.*

18. de Deene Y, de Wagter C, van Duyse BM, Derycke S, de Neve W, Achten E (1998) Three dimensional dosimetry using polymer gel and magnetic resonance imaging applied to the verification of conformal radiation therapy in head and neck cancer. *Radiother Oncol,* ***48:*** *283–291.*
19. Depuydt T, Van Esch A, Huyskens P (2002) A quantitative evaluation of IMRT dose distributions: refinement and clinical assessment of the gamma evaluation. *Radiother Oncol,* ***62:*** *309–319.*
20. Van Zijtveld M, Dirkx ML, de Boer HC, Heijmen BJ (2006) Dosimetric pre-treatment verification of IMRT using an EPID; clinical experience, *Radiotherapy and oncology,* ***81:*** *168-175.*
21. Khan RF, Ostapiak OZ, Szabo JJ (2008) An empirical model of electronic portal imager response implemented within a commercial treatment planning system for verification of intensity-modulated radiation therapy fields. *J Appl Clinical Med Phys,* ***9:*** *2807.*
22. Michalski J, Purdy J, Bruner DW, Amin M (2004) A phase III randomized study of high dose 3D-CRT/IMRT versus standard dose 3D-CRT/IMRT in patients treated for localized prostate cancer RTOG 0126 (Radiation Therapy Oncology Group).
23. Jha N, Seikaly H, Jacobs J, McEwan A, Weymuller E (2003) A phase II study of submandibular salivary gland transfer to the submental space prior to start of radiation treatment for prevention of radiation-induced xerostomia in head and neck cancer patients. RTOG 0244, Aug 03.
24. Ezzell G and Chungbin S (2001) The "overshoot" phenomenon in step-and-shoot IMRT delivery. *J Apply Clin Med Phys,* ***2:****138–148.*
25. Stell A, Li J, Zeidan O, Dempsey J (2004) An extensive log-file analysis of step-and-shoot intensity modulated radiation therapy segment delivery errors. *Med Phys,* ***31:*** *1593–1602.*
26. Grigorov G, Chow C, Barnett R (2006) Dosimetry limitations and a dose correction methodology for step-and-shoot IMRT. *Phys Med Biol,* ***51:*** *637–65.*